Reconstructing the archosaur radiation using a Middle Triassic archosauriform tooth assemblage from Tanzania (#39444)

First submission

Guidance from your Editor

Please submit by **11 Aug 2019** for the benefit of the authors (and your $200 publishing discount).

Structure and Criteria
Please read the 'Structure and Criteria' page for general guidance.

Raw data check
Review the raw data. Download from the materials page.

Image check
Check that figures and images have not been inappropriately manipulated.

Privacy reminder: If uploading an annotated PDF, remove identifiable information to remain anonymous.

Files

Download and review all files from the materials page.

8 Figure file(s)
3 Table file(s)
2 Raw data file(s)

Structure and Criteria

Structure your review

The review form is divided into 5 sections. Please consider these when composing your review:

1. **BASIC REPORTING**
2. **EXPERIMENTAL DESIGN**
3. **VALIDITY OF THE FINDINGS**
4. General comments
5. Confidential notes to the editor

📄 You can also annotate this PDF and upload it as part of your review

When ready submit online.

Editorial Criteria

Use these criteria points to structure your review. The full detailed editorial criteria is on your guidance page.

BASIC REPORTING

- Clear, unambiguous, professional English language used throughout.

- Intro & background to show context. Literature well referenced & relevant.

- Structure conforms to PeerJ standards, discipline norm, or improved for clarity.

- Figures are relevant, high quality, well labelled & described.

- Raw data supplied (see PeerJ policy).

EXPERIMENTAL DESIGN

- Original primary research within Scope of the journal.

- Research question well defined, relevant & meaningful. It is stated how the research fills an identified knowledge gap.

- Rigorous investigation performed to a high technical & ethical standard.

- Methods described with sufficient detail & information to replicate.

VALIDITY OF THE FINDINGS

- ℹ️ Impact and novelty not assessed. Negative/inconclusive results accepted. *Meaningful* replication encouraged where rationale & benefit to literature is clearly stated.

- All underlying data have been provided; they are robust, statistically sound, & controlled.

- Speculation is welcome, but should be identified as such.

- Conclusions are well stated, linked to original research question & limited to supporting results.

Standout reviewing tips

The best reviewers use these techniques

Tip	Example
Support criticisms with evidence from the text or from other sources	*Smith et al (J of Methodology, 2005, V3, pp 123) have shown that the analysis you use in Lines 241-250 is not the most appropriate for this situation. Please explain why you used this method.*
Give specific suggestions on how to improve the manuscript	*Your introduction needs more detail. I suggest that you improve the description at lines 57- 86 to provide more justification for your study (specifically, you should expand upon the knowledge gap being filled).*
Comment on language and grammar issues	*The English language should be improved to ensure that an international audience can clearly understand your text. Some examples where the language could be improved include lines 23, 77, 121, 128 – the current phrasing makes comprehension difficult.*
Organize by importance of the issues, and number your points	*1. Your most important issue* *2. The next most important item* *3. ...* *4. The least important points*
Please provide constructive criticism, and avoid personal opinions	*I thank you for providing the raw data, however your supplemental files need more descriptive metadata identifiers to be useful to future readers. Although your results are compelling, the data analysis should be improved in the following ways: AA, BB, CC*
Comment on strengths (as well as weaknesses) of the manuscript	*I commend the authors for their extensive data set, compiled over many years of detailed fieldwork. In addition, the manuscript is clearly written in professional, unambiguous language. If there is a weakness, it is in the statistical analysis (as I have noted above) which should be improved upon before Acceptance.*

Reconstructing the archosaur radiation using a Middle Triassic archosauriform tooth assemblage from Tanzania

Devin K Hoffman [Corresp., 1], **Hunter Edwards** [1, 2], **Paul M Barrett** [3], **Sterling J Nesbitt** [1]

[1] Department of Geosciences, Virginia Polytechnic Institute and State University (Virginia Tech), Blacksburg, Virginia, United States of America

[2] Department of Geological Sciences, University of Cape Town, Rondebosch, South Africa

[3] Department of Earth Sciences, Natural History Museum, London, United Kingdom

Corresponding Author: Devin K Hoffman
Email address: devinkh5@vt.edu

Following the Permo-Triassic mass extinction, Archosauriformes – the clade that includes crocodylians, birds, and their extinct relatives – rapidly diversified into numerous distinct lineages, became distributed globally, and, by the Late Triassic, filled a wide array of resource zones. Current scenarios of archosauriform evolution are ambiguous with respect to whether their taxonomic diversification in the Early–Middle Triassic coincided with the initial evolution of dietary specializations that were present by the Late Triassic, or if their ecological disparity arose sometime after lineage diversification. Late Triassic archosauriform dietary specialization is recorded by morphological divergence from the plesiomorphic archosauriform tooth condition (laterally-compressed crowns with serrated carinae and a generally triangular lateral profile). Unfortunately, the roots of this diversification are poorly documented, with few known Early–Middle Triassic tooth assemblages, limiting characterizations of morphological diversity during this critical, early period in archosaur evolution. Recent fieldwork (2007–2017) in the Middle Triassic Manda Beds of the Ruhuhu Basin, Tanzania, recovered a tooth assemblage that provides a window into this poorly sampled interval. To investigate the taxonomic composition of that collection, we built a dataset of continuous quantitative and discrete morphological characters based on *in situ* teeth of known taxonomic status (e.g., *Nundasuchus*, *Parringtonia*: N = 65) and a sample of isolated teeth (N = 31). Using crown heights from known taxa to predict tooth base ratio (= base length/base width), we created a quantitative morphospace for the tooth assemblage. The majority of isolated, unassigned teeth fall within a region of morphospace shared by several Manda taxa (e.g., *Nundasuchus*, *Parringtonia*); two isolated teeth fall exclusively within a 'Pallisteria' morphospace. A non-metric multidimensional scaling ordination (N = 67) of 11 binary characters reduced overlap between species. The majority of the isolated teeth from the Manda assemblage fall within the *Nundasuchus* morphospace. This indicates these teeth

are plesiomorphic for archosauriforms as *Nundasuchus* exhibits the predicted plesiomorphic condition of archosauriform teeth. Our model shows that even the conservative tooth morphologies of archosauriforms can be differentiated and assigned to species/genus level, rendering the model useful for identifying isolated teeth. The large overlap in tooth shape among the species present and their overall similarity indicates that dietary specialization lagged behind species diversification in archosauriforms from the Manda Beds, a pattern predicted by Simpson's 'adaptive zones' model. Although applied to a single geographic region, our methods offer a promising means to reconstruct ecological radiations and are readily transferable across a broad range of vertebrate taxa throughout Earth history.

Reconstructing the Archosaur Radiation using a Middle

Triassic Archosauriform Tooth Assemblage from Tanzania

3 Devin K. Hoffman[1], Hunter Edwards[1,2], Paul M. Barrett[3], Sterling J. Nesbitt[1]
4 [1] Department of Geosciences, Virginia Tech, Blacksburg, VA, USA
5 [2] Department of Geological Sciences, University of Cape Town, Rondebosch 7701, South Africa
6 [3] Department of Earth Sciences, Natural History Museum, London, UK
7
8 Corresponding Author:
9 Devin K. Hoffman[1]
10 926 West Campus Drive, Blacksburg, VA, 24061, USA
11 Email address: devinkh5@vt.edu

12   Following the Permo-Triassic mass extinction, Archosauriformes – the clade that includes

13   crocodylians, birds, and their extinct relatives – rapidly diversified into numerous distinct

14   lineages, became distributed globally, and, by the Late Triassic, filled a wide array of resource

15   zones. Current scenarios of archosauriform evolution are ambiguous with respect to whether

16   their taxonomic diversification in the Early–Middle Triassic coincided with the initial evolution

17   of dietary specializations that were present by the Late Triassic, or if their ecological disparity

18   arose sometime after lineage diversification. Late Triassic archosauriform dietary specialization

19   is recorded by morphological divergence from the plesiomorphic archosauriform tooth condition

20   (laterally-compressed crowns with serrated carinae and a generally triangular lateral profile).

21   Unfortunately, the roots of this diversification are poorly documented, with few known Early–

22   Middle Triassic tooth assemblages, limiting characterizations of morphological diversity during

23   this critical, early period in archosaur evolution. Recent fieldwork (2007–2017) in the Middle

24   Triassic Manda Beds of the Ruhuhu Basin, Tanzania, recovered a tooth assemblage that provides

25   a window into this poorly sampled interval. To investigate the taxonomic composition of that

26   collection, we built a dataset of continuous quantitative and discrete morphological characters

27   based on *in situ* teeth of known taxonomic status (e.g., *Nundasuchus*, *Parringtonia*: N = 65) and

28   a sample of isolated teeth (N = 31). Using crown heights from known taxa to predict tooth base

29   ratio (= base length/base width), we created a quantitative morphospace for the tooth

30   assemblage. The majority of isolated, unassigned teeth fall within a region of morphospace

31   shared by several Manda taxa (e.g., *Nundasuchus*, *Parringtonia*); two isolated teeth fall

32   exclusively within a '*Pallisteria*' morphospace. A non-metric multidimensional scaling

33   ordination (N = 67) of 11 binary characters reduced overlap between species. The majority of the

34   isolated teeth from the Manda assemblage fall within the *Nundasuchus* morphospace. This

35   indicates these teeth are plesiomorphic for archosauriforms as *Nundasuchus* exhibits the

36   predicted plesiomorphic condition of archosauriform teeth. Our model shows that even the

37   conservative tooth morphologies of archosauriforms can be differentiated and assigned to

38   species/genus level, rendering the model useful for identifying isolated teeth. The large overlap

39   in tooth shape among the species present and their overall similarity indicates that dietary

40   specialization lagged behind species diversification in archosauriforms from the Manda Beds, a

41   pattern predicted by Simpson's 'adaptive zones' model. Although applied to a single geographic

42   region, our methods offer a promising means to reconstruct ecological radiations and are readily

43   transferable across a broad range of vertebrate taxa throughout Earth history.

Introduction

45 Adaptive radiations, or evolutionary diversifications, play a critical role in the history of life as

46 clades speciate and fill new ecological roles over geologically rapid time intervals (Simpson,

47 1944; Schluter, 1996). Although there are examples of adaptive radiations that are not speciose

48 (e.g. Darwin's finches), or adaptively disparate (e.g. crotaphytine and oplurine iguanids), such a

49 framework is still useful for structuring macroevolutionary questions and explaining present (and

50 past) biological diversity (Gavrilets and Losos, 2009). Adaptive radiations and the shifts in

51 evolutionary rates associated with them are among the most studied aspects of evolutionary

52 biology (e.g. Stanley, 1979; Losos and Miles, 1994, 2002; Gavrilets and Losos, 2009; Revell et

53 al., 2018; Slater and Friscia, 2019). However, empirical uncertainties remain regarding many of

54 the properties of adaptive radiations (Gavrilets and Losos, 2009; Slater and Friscia, 2019), with

55 the relative timings of lineage diversification and ecological disparity during adaptive radiations

56 being one such problem. Does lineage diversification come first, followed by specialization and

57 evolution within an 'adaptive zone' (Simpson, 1944, 1953) or does ecological specialization

58 drive lineage diversification simultaneously (Schluter, 1996)? In the former case species fill the

59 same resource zones using similar, ancestral morphological structures (e.g. identical tooth

60 morphologies), whereas in the latter each species would be expected to have a unique, derived

61 morphology for its resource zone at the start of the radiation (for an empirical example, see

62 Slater and Friscia, 2019). Determining which of these competing hypotheses operated in a

63 particular case requires us to reconstruct an evolutionary radiation where a species-poor,

64 adaptively constrained clade diversifies into a species-rich, adaptively disparate clade.

65   One such radiation occurred during the Triassic Period, following the Permo-Triassic

66 mass extinction (PTME: Raup, 1979; Erwin, 1994; Chen and Benton, 2012; Benton and Newell,

67   2014) as archosauriforms recovered, rapidly diversified, and spread across Pangea to dominate

68   terrestrial ecosystems for the next 150 million years (Nesbitt, 2011; Ezcurra and Butler, 2018). In

69   addition to Archosauriformes being a speciose and disparate radiation, they also provide an

70   opportunity to test adaptive radiations at a higher phylogenetic level. Lineage diversification of

71   archosaurs was rapid after the PTME, and by the Middle Triassic many non-archosaurian

72   archosauriform and crown archosaur clades had appeared (Ezcurra, 2016; Foth et al., 2016;

73   Ezcurra and Butler, 2018). By the Late Triassic archosaurs filled a wide variety of ecological

74   roles, from top predators to large herbivores, and were represented in terrestrial, freshwater, and

75   even marine ecosystems (e.g. Li et al., 2006; Butler et al., 2019). If lineage diversification occurs

76   first, followed by subsequent ecological disparity, we would expect Middle Triassic

77   archosauriforms from across the tree to present a limited range of ecologies. The question that

78   arises is how best to measure ecological disparity? Ecological disparity covers a variety of

79   physiological, behavioral, and morphological traits but the nature of the fossil record limits its

80   measure primarily to morphology. Previous work has used cranial morphology as a measure of

81   disparity (e.g. Foth et al., 2016); however complete, or even partial, skulls are rare for Early–

82   Middle Triassic archosauriforms. Therefore, an alternative morphological system to approximate

83   ecological disparity is needed. In this study we use teeth as an indicator of ecological disparity

84   because they have relatively high preservation potential (e.g. Turner-Walker, 2008) and offer a

85   direct link to ecology through diet (Lucas, 1979; Dessem, 1985; Scallon and Shine, 1988;

86   Sander, 1997; Linde, Palmer & Gómez-Zurita, 2004; Santana, Strait & Dumont, 2011;

87   Zahradnicek et al., 2014). We consider diet as the aspect of ecology of interest for both the

88   relative ease of inference from morphology alone and the use of diet in previous studies of

89   evolutionary radiations (e.g. Slater and Friscia, 2019).

90   Although tooth assemblages are rare in Middle Triassic terrestrial settings, recent

91 fieldwork (2007, 2008, 2012, 2015, 2017) in the Manda Beds of the Ruhuhu Basin, Tanzania

92 (Sidor and Nesbitt, 2017), has revealed a rich assemblage of archosauriforms known from

93 postcrania and partial crania, including teeth (e.g. Nesbitt et al., 2010; 2014; Smith et al., 2018).

94 Specifically, these teeth come from the middle and upper Lifua Member bone accumulations

95 (Smith et al., 2018), which are thought to be Anisian in age (Rubidge, 2005) but may be as

96 young as early Carnian (Ottone et al., 2014; Marsicano et al., 2016; Wynd et al., 2018; Peecook

97 et al., 2018). If the Anisian age is correct, then this is one of the oldest, diverse archosaur faunas

98 known that is also represented by specimens from historical collections (e.g. Butler et al., 2009;

99 2017; Nesbitt et al., 2010; 2013; 2014; 2017; Barrett, Nesbitt & Peecook, 2015). Using a

100 combination of information from these new and historical collections, we quantify tooth

101 disparity in this earliest part of the archosaur radiation to generate a morphospace visualization.

102 From this we can assign isolated teeth to specific taxon, visualize inter- and intraspecific

103 variation as well as intra-individual variation, and use this variation as a window into the

104 ecological disparity of the archosauriforms within the Lifua Member assemblage. To achieve

105 these goals, we use a combination of *in situ* teeth from jaw elements assignable to particular

106 species (Figure 1), and isolated teeth attributable to Archosauriformes (Figure 2). Of particular

107 interest is whether the isolated teeth fall within, or expand, the region of morphospace occupied

108 by the described Manda Beds taxa.

109 *Institutional Abbreviations* – **NHMUK**, Natural History Museum, London, U.K.; **NMT**,

110 National Museum of Tanzania, Dar es Salaam, Tanzania.

111

112 **Materials & Methods**

113   The 31 isolated teeth included in this study were all collected from surface accumulations

114   of vertebrate fossils during fieldwork in 2007, 2008, 2012, 2015, and 2017 from the Manda Beds

115   of the Ruhuhu Basin by a multi-institutional team (Sidor and Nesbitt, 2017). All of the isolated

116   teeth included in this study are currently housed at Virginia Tech Department of Geosciences and

117   will be permanently reposited and managed in the National Museum of Tanzania. In addition to

118   these isolated teeth (seven of which were referred to *Nundasuchus*: see Nesbitt et al., 2014), we

119   also included teeth from within the tooth-bearing elements of five taxonomically distinct

120   archosauriforms from the Manda Beds: *Nundasuchus* (NMT RB48), *Parringtonia* (NMT

121   RB426), *Asilisaurus* (NMT RB837), '*Pallisteria*' (NHMUK PV R36620), and one currently

122   undescribed pseudosuchian that we refer to –by its specimen number (NMT RB187). We assign

123   the isolated teeth to Archosauriformes on the basis of their serration morphology (Nesbitt, 2011)

124   as well as their general ziphodont construction, including lateral compression (e.g. Godefroit and

125   Cuny, 1997).

126   To quantify tooth shape, linear measurements (total crown height, base width, and fore-

127   aft base length) and denticle counts were made following the protocol in Smith, Vann & Dodson

128   (2005), although due to the smaller size of the teeth in our study, we used 1 mm denticle

129   densities, rather than 5 mm densities (Supplementa1 Data S1). All statistical analyses were

130   performed in R (v 3.1.2) and the RStudio console (v 1.1.383). All graphs of quantitative data

131   were made using the R package "ggplot2" (Wickham, 2009). To capture tooth disparity (from

132   log-transformed linear measurements) we used sum of variances with 95% predictive intervals

133   following the methodology of Larson, Brown & Evans (2016). We chose to use sum of variances

134   as our measure of disparity due to its prevalence in the literature and its robustness when

135   working with small sample sizes. Sample size varied from 2–14 teeth, however, sample size does

136   not significantly affect the sum of variance analysis (Ciampaglio, Kemp, & McShea, 2001). In

137   *Asilisaurus* the 14 teeth largely contributed base and width measurements because only three

138   teeth were complete enough to measure crown height. We constructed a linear model in R

139   predicting the variable of tooth base shape (ratio of mesiodistal length over labiolingual width)

140   by the variables of total crown height and species-level assignment such that base shape = total

141   crown height * species assignment. The effects of each species on predicting tooth base shape

142   were elucidated using the R package "lsmeans" (Lenth, 2016) using a pairwise comparison in the

143   model by taxon. We plotted the teeth of known taxonomic affinity using ggplot2 (Wickham,

144   2009) to produce a base morphospace into which we plotted results from the isolated teeth for

145   comparison.

146   Simple quantitative measurements only capture the overall shape of the teeth, and all of

147   the teeth in the study resemble the hypothetical ancestral archosauriform tooth (serrated,

148   recurved, and laterally compressed: Nesbitt, 2011). In order to more fully capture and describe

149   the subtle variation of these teeth, a method of capturing discrete variation is needed. Non-metric

150   multidimensional scaling (NMDS) is an ordination method that visualizes variation that can

151   incorporate discrete qualitative features. We created a set of 11 binary characters for scoring

152   isolated and *in situ* teeth for NMDS (Table 1, Figure 3, Supplemental Data S2). All characters

153   except one are new to this analysis (trait 6, dental caudae = shallow grooves extending from

154   between two adjacent denticles present/absent is taken from Abler [1992]). None of the traits

155   used in this study have been used in phylogenetic analyses of archosauriforms, in order to avoid

156   circular reasoning when comparing our ecological signal to taxonomic and clade identity. The

157   NMDS analysis was conducted in PAST (Hammer, Harper & Ryan, 2001) with a Bray-Curtis

158   transformation. We ran an additional NMDS analysis in PAST using average taxon and

159   morphotype scores where traits were scored for each taxon with >50% agreement of *in situ* teeth.

160   Traits for which <50% of the specimens in the taxon or morphotype were scored as unknown

161   ("?").

162

163   **Isolated Tooth Descriptions**

164   *Morphotype A:* These teeth (Figure 2A) are generally triangular in outline in lateral view and

165   most are recurved (the point of the crown is distal to the distal-most extent of the crown base)

166   although the remainder have crown tips that are level with the distal-most extent of the crown

167   base. The labial and lingual sides of the crown lack ridges (i.e. no fluting), and the labial side of

168   the crown exhibits greater convexity than the lingual side. The mesial denticle series terminates

169   more apically along the crown margin than the distal series, which continues along the entire

170   height of the crown though both start at the tip of the crown. The mesial denticle series is also

171   offset from the mesial-distal long axis of the crown base, deflecting to the lingual side toward the

172   crown base. The denticle densities range from 2–5 per mm. Denticle caudae (Abler, 1992),

173   which are shallow grooves extending from between two adjacent denticles, are often present and

174   directed parallel to the denticles. These denticle caudae are most easily viewed in mesial or distal

175   view (Figure 3F).

176   In general, Morphotype A teeth strongly resemble both *in situ* and isolated teeth of

177   *Nundasuchus* (Figure 1; Nesbitt et al., 2014). Particularly important features are the presence of

178   denticle caudae, an unequal labial-lingual curvature, and the more apical termination of the

179   mesial denticle series relative to the distal denticle series. Also like *Nundasuchus*, teeth of

180   Morphotype A exhibit a mix of states in the changing curvature of the mesial crown edge in

181   lateral view, with some teeth gradually changing angles and others exhibiting an abrupt shift in

182 angle. The *in situ* teeth of *Nundasuchus* can exhibit either state depending on the proximity of

183 the mesial edge of the crown to the distal edge of the preceding tooth. Though this combination

184 of traits is only found in *Nundasuchus* in the Manda Beds fauna, archosauriforms from the

185 Middle and Upper Triassic elsewhere (e.g. de Oliveira and Pinheiro, 2017; Schoch et al., 2018).

186 *Morphotype B:* These teeth (Figure 2B) are triangular in shape in lateral view and are

187 occasionally recurved, although in most the apical tip of the crown is approximately level with

188 the distal-most end of the crown base. Morphotype B tooth crowns lack fluting and, in contrast to

189 Morphotype A, the labial and lingual curvatures are equal. None of the teeth are bulbous (no

190 labiolingual measurements are greater than crown base width). In the majority of Morphotype B

191 teeth the mesial margin of the crown possesses a single point where the angle of the mesial

192 carina changes abruptly. As in Morphotype A teeth, the mesial series of denticles in Morphotype

193 B teeth terminates on the crown further apically than the distal series, which often terminates at

194 the crown base. However, the mesial row of denticles is in line with the mesial-distal long axis of

195 the crown base. The denticle densities range from 3–8 per mm. Denticle caudae are present on

196 some of the teeth and are directed parallel to the denticles. Although these teeth bear a strong

197 resemblance to Morphotype A, they can be differentiated by their equal labial and lingual

198 curvatures. Morphotype B teeth are similar to some of the *in situ* and isolated *Nundascuhus* teeth

199 (Figure 1,2; Nesbitt et al., 2014).

200 *Morphotype C:* This morphotype (Figure 2C) is represented by a single tooth in our assemblage,

201 NMT RB831. The overall shape is tall, near conical, and recurved. The crown lacks fluting and

202 the labial curvature is greater than the lingual curvature. Although its labial-lingual curvature is

203 unequal, the mesial denticle series is positioned along the midline of the mesial-distal long axis.

204 The orientation of the mesial edge of the tooth changes gradually, forming a long, continuous

205   curve. The tooth is not bulbous. Denticle densities range from 2–4 per mm, and no denticle

206   caudae are present. There is no variation in either the shape or size of the denticles between the

207   mesial and distal series or along the length of the crown. Unlike either Morphotypes A or B, the

208   mesial series of denticles in Morphotype C ends at approximately the same level on the crown as

209   the distal series, just above the crown base.

210   In general size and shape, as well as in many of its discrete features, the Morphotype C

211   tooth is similar to the teeth of '*Pallisteria*' based on our observations. The teeth of the latter

212   taxon are large, conical, recurved, and possess unequal labial-lingual curvature. The denticle

213   density is low (< 3 per mm) in the middle part of the tooth crown and denticles show little

214   variation in shape or size. Unfortunately, none of the '*Pallisteria*' teeth could be scored for Trait

215   7 (termination height of the mesial denticle series; Table 1) due to poor preservation of the

216   denticles, which otherwise differentiates Morphotype C teeth from morphotypes A and B. If

217   Morphotype C is similar to, or is, '*Pallisteria*', then subsequent '*Pallisteria*' tooth discoveries

218   should be expected to have sub-equally extending mesial and distal denticle rows.

219

220   ***In situ* Tooth Descriptions**

221   *Nundasuchus*: We included a total of 13 *Nundasuchus* teeth, six *in situ* and seven isolated,

222   originally described in Nesbitt et al. (2014). The teeth range in height from 5.6 to 22 mm with

223   denticle densities from 2–5 per mm. All the teeth are labio-lingually compressed and are serrated

224   on both mesial and distal margins. Only one tooth possesses a recurved tip that extends past the

225   distal-most end on the tooth base. Most teeth are smooth on the sides with a single exception

226   exhibiting fluting. All of the teeth possess: unequal labial-lingual curvatures, a mesial row of

227   denticles that terminates higher on the tooth crown than the distal row of denticles, and a mesial

228   carina that is offset from the midline. Only two of the teeth possess dental caudae and one tooth

229   is bulbous. In some teeth the mesial and distal denticle rows differ in size and/or in shape. About

230   half the teeth have a distinct point on the mesial margin where the angle of the edge changes

231   abruptly. For the *in situ* teeth this seems to be related to how close the tooth is to the preceding

232   socket, with the closer the distance being associated with an abrupt angle shift point.

233   *Asilisaurus*: We included 14 *in situ* teeth though only three of these included more than the very

234   base of the tooth. These three ranged in height from 1.6 to 2.9 mm and had a denticle density of

235   ~8 per mm. The teeth are closely packed, ankylosed to the sockets, and peg-like in shape

236   (Nesbitt et al., 2010). All of the teeth have: smooth sides, equal labial-lingual curvature, and

237   subeven mesial and distal row of denticles. None of the *Asilisaurus* teeth possess dental caudae

238   and the mesial edge of the teeth changes angles gradually.

239   *Parringtonia*: Of the 14 teeth in the study, 12 were *in situ* and the other two larger, isolated teeth.

240   The teeth range in size from 2.5–21.6 mm, though the tallest *in situ* tooth is 8.3 mm, and the

241   denticle densities vary from 5–15 per mm. Most of the *Parringtonia* teeth lacked crown tips,

242   though the two complete teeth are not recurved. All of the teeth are labio-lingually compressed

243   and possess fluting and a mesial carina along the midline. The mesial and distal denticle series of

244   all the teeth remain constant in both shape and size, though the mesial denticle series terminates

245   higher on the crown than the distal series. In all the teeth the mesial edge angle changes

246   gradually.

247   NMT RB187: All 13 teeth of the teeth included from NMT RB187 are *in situ*. The labio-

248   lingually compressed teeth range from 5.3–13.4 mm tall with denticle densities of 8–14 per mm.

249   All of the teeth are recurved, fluted, and lack dental caudae. The mesial edge of the teeth changes

250   gradually and follows the mesial-distal long axis. In teeth with preserved crown tips the shape of

251   the denticles remains constant. Of all the taxa included here, NMT RB187 exhibits the greatest

252   degree of recurvedness.

253   '*Pallisteria*': We included 11 *in situ* teeth from the left and right maxillae of '*Pallisteria*'. These

254   teeth are the largest of all the taxa, ranging from 36.1–70.3 mm, and have the lowest density,

255   from 2–3 per mm. All except one are recurved and all have smooth crowns and lack dental

256   caudae. Most of the teeth have uneven labial-lingual curvature and a mesial edge that changes

257   angles gradually. The mesial carina is offset from the mesiodistal long axis in most the teeth and

258   the denticles remains constant in shape and size along the height of the crown.

259

260   **Results**

261   For our linear model we predicted the tooth base shape (ratio of labiolingual base width

262   to mesiodistal base length) using the total apicobasal crown height and the taxonomic affinity of

263   the tooth (base ~ tch + taxon) with the lm() command in base R (Table 2). We found that tooth

264   height was not a significant predictor of base shape (p = 0.0933. We used the R package

265   "lsmeans" to further investigate the differences between the species' tooth shape (Table 3). From

266   this metric NMT RB187 has a significantly higher base shape ratio than all other taxa except

267   *Parringtonia* (p = 0.3788).

268   The sum of variances analysis (Figure 4) included all known Manda Beds archosauriform

269   taxa with associated dentition and two of the three morphotypes, as only a single tooth of

270   Morphotype C is present in our assemblage. These variances provide a quantification of

271   intraspecific variation in tooth size and shape, and allow for an equal interspecific comparison.

272   Mean variances ranged from a low of 0.02 log units in '*Pallisteria*', two large isolated teeth of

273   *Parringtonia*, and Morphotype B, to a high of 0.145 log units in Morphotype A (Figure 4).

274   More useful for visualizing variation than the linear model and lsmeans contrasts are

275   morphospace plots of the teeth from our generically determinate specimens, with the isolated,

276   unidentified teeth added for comparison. There is much overlap in morphospace occupancy,

277   particularly on the left side (shorter height) portion of the graph, although *'Pallisteria'* occupies

278   its own section of morphospace in taller crown heights (Figure 5). Teeth towards the bottom of

279   the morphospace (lower base ratio) are more rounded and cone-like, whereas those with higher

280   base ratios are more laterally compressed. With size alone two of the Morphotype A teeth fall in

281   *'Pallisteria'* morphospace and the Morphotype C tooth with *Nundasuchus* morphospace contrary

282   to the discrete descriptive predictions. The relationship between base width and mesiodistal base

283   length provides little more distinction of the taxa included, and the impact of crown size is still

284   evident (Figure 6). In general the ratio of base mesiodistal length and labiolingual width follows

285   a linear trend controlled by size.

286   A total of 21 isolated teeth and 46 *in situ* teeth of known affinity were complete enough

287   to be scored for the NMDS analysis. Convex hulls are more differentiated than in the quantitative

288   morphospace, with almost no overlap of *Nundasuchus* with either NMT RB187 or *Parringtonia*

289   (Figure 7). Overlap of NMT RB187 and *Parringtonia* remains, but most of the isolated teeth fall

290   exclusively within or adjacent to the zone of *Nundasuchus* and *'Pallisteria'* (Figure 7). The high

291   degree of overlap between *Parringtonia* and NMT RB187 likely reflects their often-shared

292   feature of having parallel ridges (fluting) along the labial and lingual sides of the tooth crown.

293   The only other tooth in the study with fluting is a single example referred to *Nundasuchus*. The

294   use of taxa and morphotype 'averages' in traits reveals similar groupings to the complete dataset,

295   with average morphotype scores between those of known taxa (Figure 8).

296

297   **Discussion**

298   We present the first quantitative description of a Middle Triassic archosauriform tooth

299   assemblage, which reveals substantial conservation of tooth morphology at the beginning of the

300   archosaur radiation. Intraspecific variation appears to be as great, if not greater, than interspecific

301   variation. Morphotype A displays the greatest variance in tooth size in the sample, although

302   *Nundasuchus* has a very similar sum of variance structure (Figure 4). Driving at least part of the

303   pattern we see in our disparity analysis is whether more than a single individual of a given taxon

304   is included in our study. For example, NMT RB187, '*Pallisteria*', and *Parringtonia* all display

305   low disparity, but our sample includes only elements from a single individual of each taxon,

306   whereas the *Nundasuchus* sample includes *in situ* teeth from one lower jaw (the holotype

307   specimen) and associated isolated teeth assigned to the holotype (Figure 4). Although two of the

308   isolated teeth from our assemblage fall exclusively within the '*Pallisteria*' quantitative

309   morphospace, most of the isolated teeth fall within a zone of overlap between *Nundasuchus*,

310   NMT RB187, and *Parringtonia* (Figure 5). Much of this quantitative variation reflects body size

311   (Figure 6). *Nundasuchus* and '*Pallisteria*' are much larger than the other taxa, which helps to

312   differentiate their morphospace from that of smaller-bodied taxa. *Asilisaurus* is the smallest

313   taxon in our sample, but there is postcranial evidence of a larger silesaurid in the Lifua

314   assemblage (possibly a very large individual of *Asilisaurus*; Barrett, Nesbitt, & Peecook, 2015)

315   that would be comparable in size to *Nundasuchus* and '*Pallisteria*'. Recovery of teeth from

316   silesaurid individuals of this larger size might reduce some of the differentiation between them,

317   *Nundasuchus*, and '*Pallisteria*' though we would still expect silesaurid teeth to be smaller

318   relative to the same body size.

319   The NMDS ordination improves the differentiation of taxa, with *Asilisaurus* and the

320   large-bodied predator '*Pallisteria*' more clearly separated from the still overlapping undescribed

321   pseudosuchian, and *Parringtonia* and *Nundasuchus* exhibiting wide variation in morphospace

322   overall, bridging the space between all taxa, and overlapping a substantial part of '*Pallisteria*'

323   morphospace (Figure 7). These results identify two general areas of morphospace, one shared by

324   the undescribed pseudosuchian and *Parringtonia* and the other by *Nundasuchus* and

325   '*Pallisteria*'. The teeth of *Parringtonia* and the undescribed pseudosuchian share several

326   features, notably presence of fluting, a mesial carina along the midline tooth axis, and a high

327   denticle density ($\geq$ 3 per mm). By contrast, *Nundasuchus* and '*Pallisteria*' teeth lack fluting,

328   possess an offset mesial carina, unequal labial/lingual curvature, and have a low denticle density

329   ($<$ 3 per mm). This result is further supported when the average or typical score of each taxon is

330   used, with NMT RB187, *Asilisaurus*, and *Parringtonia* clustering together versus *Nundasuchus*

331   and '*Pallisteria*' on the other side of morphospace (Figure 8). Given that many of the isolated

332   teeth resemble those of *Nundasuchus*, it is not surprising that most of the isolated teeth fall

333   within the convex hull defined by *Nundasuchus* (Figure 7). We cannot, however, definitely

334   assign these teeth to *Nundasuchus* due to the overlap in discrete characters among our included

335   taxa.

336   Our results using both methods demonstrate that many of the isolated teeth resemble

337   those from currently recognized taxa. However, several teeth fall outside of the morphospace

338   defined by known taxa and could indicate either intraspecific variation (due to heterodonty or

339   ontogeny) or could represent other, as yet unsampled, taxa. Our methodologies are flexible and

340   the datasets can incorporate additional specimens as they are excavated, so these approaches

341   could be applied to other tooth assemblages throughout the Triassic across a broad range of

342   spatial, temporal, and taxonomic scales.

343   **Ecological Differentiation.** There are some hints of dietary separation between large-

344   and small-bodied archosaurs based on minor changes in tooth morphology and consideration of

345   body size. However, our results, which show high degrees of overlap in tooth morphology

346   suggest that ecological differentiation, at least in diet, appears to lag behind lineage

347   diversification, at least with respect to Manda archosauriforms. Four of the five recognized taxa

348   included here possess ziphodont dentitions (=labiolingual narrow crown [labiolingual width <

349   60% of mesiodistal length], recurved, typically serrated carinae, and no constriction at the cervix

350   *sensu* Hendrickx, Mateus & Araújo, 2015) indicative of a carnivorous diet. Only *Asilisaurus*

351   differs in possessing a conidont dentiton (=conical crowns with small denticles or no denticles,

352   and typically fluted *sensu* Hendrickx, Mateus & Araújo, 2015). Conidonty is present in

353   spinosaurids, many crocodylians, marine reptiles, and pterosaurs (Hendrickx, Mateus & Araújo,

354   2015) and has been linked to piscivory. Following this criterion *Asilisaurus* would be categorized

355   as a potential piscivore. However, dietary reconstructions of *Silesaurus opolensis*, another

356   silesaurid possessing similar dentition to *Asilisaurus*, have been herbivorous or omnivorous

357   based upon dental microwear (Kubo and Kubo, 2014) or insectivorous based upon coprolites

358   (Qvarnström et al., 2019). Thus, in the Manda Beds tooth assemblage there are two large-bodied

359   carnivores (*Nundasuchus* and '*Pallisteria*'), two small-bodied carnivores (*Parringtonia* and an

360   undescribed pseudosuchian), and one small-bodied, non-carnivore (*Asilisaurus*). The Middle

361   Triassic Manda Beds may, therefore, be capturing the beginning of the 'Explosive Phase' of

362   Simpson's (1944) theoretical model as lineages split and begin to move towards new adaptive

363   zones. Further tooth assemblages will need to be evaluated to see if this is a broader trend that

364 holds across the Triassic archosaur radiation. We posit that the qualitative NMDS ordination

365 method gives us the necessary lens for testing this hypothesis.

366

367 **Conclusions**

368   Simple quantitative measures of tooth shape were of limited use in characterizing the

369 Middle Triassic Manda Beds archosauriform tooth assemblage because of the highly conserved

370 morphology of many specimens. Instead, an ordination based on discrete characters provided a

371 more effective means of differentiating the teeth of distinct taxa. Nevertheless, we found little

372 evidence for significant ecological differentiation of tooth shape between the five taxa included

373 in our study. Most isolated teeth (n = 17/21) fall within the spectrum of recognized taxon

374 variation, and the remainder represent either unsampled taxa or unsampled intraspecific

375 variation.

376   Our relatively simple metrics can be used to describe subtle differences in tooth

377 morphology. These objective methods for grouping teeth provide a complimentary method for

378 assigning teeth to dietary roles, a practice that typically relies on qualitative comparisons to the

379 teeth of extant taxa of known diet (e.g. Fraser and Walkden, 1983; Sander, 1999; Barrett, 2000;

380 Hungerbühler, 2000) or other fossil taxa (e.g. Dzik, 2003; Hendrickx, Mateus & Araújo, 2015;

381 de Oliveira and Pinheiro, 2017). Furthermore, the methods applied herein provide an evaluation

382 of ecological disparity that is separate from the features used in phylogenetic analyses, so that we

383 can compare these two evolutionary phenomena independently. This method is readily

384 transferable to tooth assemblages from other localities pertaining to any vertebrate clade. Our

385 next step will be to apply this technique to richer Middle Triassic sites, as well as Late Triassic

386   sites, to understand how morphological and ecological diversity changed during the early stages

387   of the archosaur radiation.

388

389   **Acknowledgments**

390   We thank Dr. Kate Langwig and Dr. Josef Uyeda for their assistance and advice with R Studio,

391   and the Virginia Tech Paleobiology Research Group for helpful comments.

392 **Works Cited**

393 Abler, W. L., 1992, The serrated teeth of tyrannosaurid dinosaurs, and biting structures in other

394   animals: Paleobiology, v. 18, no. 2, p. 161-183.

395 Barrett, P. M., 2000, Prosauropods and iguanas: speculation on the diets of extinct reptiles. In

396   Sues HD, ed. *Evolution of Herbivory in Terrestrial Vertebrates: Perspectives from the*

397   *Fossil Record*. Cambridge: Cambridge University Press, 42-78.

398 Barrett, P. M., Nesbitt, S. J., and Peecook, B. R., 2015, A large-bodied silesaurid from the Lifua

399   Member of the Manda beds (Middle Triassic) of Tanzania and its implications for body-

400   size evolution in Dinosauromorpha: Gondwana Research, v. 27, p. 925-931.

401 Benton, M. J., and Newell, A. J., 2014, Impacts of global warming on Permo-Triassic terrestrial

402   ecosystems: Gondwana Research, v. 25, p. 1308-1337.

403 Butler, R. J., Barrett, P. M., Abel, R. L., and Gower, D. J. 2009. A possible ctenosauriscid

404   archosaur from the Middle Triassic Manda Beds of Tanzania: Journal of Vertebrate

405   Paleontology, v. 29, no. 4, p. 1022-1031.

406 Butler, R. J., Nesbitt, S. J., Charig, A. J., Gower, D. J., and Barrett, P. M., 2017, *Mandasuchus*

407   *tanyauchen*, gen. et sp. nov., a pseudosuchian archosaur from the Manda Beds (?Middle

408   Triassic) of Tanzania: Journal of Vertebrate Paleontology, v. 37, no. sup1, p. 96-121.

409 Butler, R. J., Jones, A. S., Buffetaut, E., Mandl, G. W., Scheyer, T. M., and Schultz, O. 2019.

410   Description and phylogenetic placement of a new marine species of phytosaur

411   (Archosauriformes: Phytosauria) from the Late Triassic of Austria: Zoological Journal of

412   the Linnean Society, zlz014, https://doi.org/10.1093/zoolinnean/zlz014.

413 Chen, Z.-Q., and Benton, M. J., 2012, The timing and pattern of biotic recovery following the

414   end-Permian mass extinction: Nature Geoscience, v. 5, p. 375.

415   Ciampaglio, C.N., Kemp, M., and McShea, D.W., 2001, Detecting changes in morphospace

416   occupation patterns in the fossil record: characterization and analysis of measures of

417   disparity: Paleobiology, v. 27, p. 695-715.

418   de Oliveira, T. M., and Pinheiro, F. L., 2017, Isolated archosauriform teeth from the Upper

419   Triassic Candelária Sequence (Hyperodapedon Assemblage Zone, Southern Brazil):

420   Revista Brasileira de Paleontologia, v. 20, p. 155-162.

421   Dessem, D. 1985. Ontogenetic changes in the dentition and diet of *Tupinambis* (Lacertilia:

422   Teiidae). Copeia, v. 1985, no. 1, p. 245-247.

423   Dzik, J., 2003, A beaked herbivorous archosaur with dinosaur affinities from the early Late

424   Triassic of Poland: Journal of Vertebrate Paleontology, v. 23, p. 556-574.

425   Erwin, D. H., 1994, The Permo–Triassic extinction: Nature, v. 367, p. 231.

426   Ezcurra, M. D., 2016, The phylogenetic relationships of basal archosauromorphs, with an

427   emphasis on the systematics of proterosuchian archosauriforms: PeerJ, v. 4, p. e1778.

428   Ezcurra, M. D., and Butler, R. J., 2018, The rise of the ruling reptiles and ecosystem recovery

429   from the Permo-Triassic mass extinction: Proc R Soc Lond B Biol Sci, v. 285, no. 1880,

430   p. 20180361.

431   Foth, C., Ezcurra, M. D., Sookias, R. B., Brusatte, S. L., and Butler, R. J., 2016, Unappreciated

432   diversification of stem archosaurs during the Middle Triassic predated the dominance of

433   dinosaurs: BMC Evolutionary Biology, v. 16, no. 1, p. 188.

434   Fraser, N. C., and Walkden, G. M., 1983, The ecology of a Late Triassic reptile assemblage from

435   Gloucestershire, England: Palaeogeography, Palaeoclimatology, Palaeoecology, v. 42, p.

436   341-365.

437   Gavrilets, S., and Losos, J. B., 2009, Adaptive Radiation: Contrasting Theory with Data:

438   Science, v. 323, no. 5915, p. 732-737.

439   Godefroit, P., and Cuny, G. 1997. Archosauriform teeth from the upper Triassic of Saint-

440   Nicolas-de-Port (northeastern France): Palaeovertebrata, 26(1-4), 1-34.

441   Griffin, C. T., and Nesbitt, S. J., 2016, The femoral ontogeny and long bone histology of the

442   Middle Triassic (?late Anisian) dinosauriform *Asilisaurus kongwe* and implications for

443   the growth of early dinosaurs: Journal of Vertebrate Paleontology, v. 36, no. 3.

444   Grossnickle, D. M., and Polly, P. D., 2013, Mammal disparity decreases during the Cretaceous

445   angiosperm radiation: Proceedings of the Royal Society of London B: Biological

446   Sciences, v. 280, no. 1771, p. 20132110.

447   Hammer, Ø., Harper, D., and Ryan, P., 2001, PAST-Palaeontological statistics: Palaeontologia

448   Electronica, v. 25, no. 07, p. 2009.

449   Hendrickx, C., Mateus, O., and Araújo, R. 2015, A proposed terminology of theropod teeth

450   (Dinosauria, Saurischia): Journal of Vertebrate Paleontology, v. 35, no. 5, e982797.

451   Hungerbühler, A., 2000, Heterodonty in the European phytosaur *Nicrosaurus kapffi* and its

452   implications for the taxonomic utility and functional morphology of phytosaur dentitions:

453   Journal of Vertebrate Paleontology, v. 20, p. 31-48.

454   Kubo, T., and Kubo, M. O., 2014, Dental microwear of a Late Triassic dinosauriform, *Silesaurus*

455   *opolensis*: Acta Palaeontologica Polonica, v. 59, p. 305-313.

456   Larson, D. W., 2008, Diversity and variation of theropod dinosaur teeth from the uppermost

457   Santonian Milk River Formation (Upper Cretaceous), Alberta: a quantitative method

458   supporting identification of the oldest dinosaur tooth assemblage in Canada: Canadian

459   Journal of Earth Sciences, v. 45, no. 12, p. 1455-1468.

460 Larson, D. W., and Currie, P. J., 2013, Multivariate analyses of small theropod dinosaur teeth

461 and implications for paleoecological turnover through time: PLoS One, v. 8, no. 1, p.

462 e54329.

463 Larson, D. W., Brown, C. M., and Evans, D. C., 2016, Dental disparity and ecological stability in

464 bird-like dinosaurs prior to the end-Cretaceous mass extinction: Current Biology, v. 26,

465 no. 10, p. 1325-1333.

466 Lenth, R. V., 2016, Least-Squares Means: The R Package lsmeans. Journal of Statistical

467 Software, v. 69, no. 1, 1-33. doi:10.18637/jss.v069.i01

468 Li, C., Wu, X.-c., Cheng, Y.-n., Sato, T., and Wang, L., 2006, An unusual archosaurian from the

469 marine Triassic of China: Naturwissenschaften, v. 93, no. 4, p. 200-206.

470 Lucas, P.W. 1979. The dental-dietary adaptations of mammals: Neues Jahrbuch für Geologie und

471 Paläontologie, Monatshefte, v. 8, p. 486–512.

472 Linde, M., Palmer, M., and Gómez-Zurita, J. 2004, Differential correlates of diet and phylogeny

473 on the shape of the premaxilla and anterior tooth in sparid fishes (Perciformes: Sparidae):

474 Journal of Evolutionary Biology, v. 17, no. 5, p. 941-952.

475 Marsicano, C. A., Irmis, R. B., Mancuso, A. C., Mundil, R., and Chemale, F., 2016, The precise

476 temporal calibration of dinosaur origins: Proceedings of the National Academy of

477 Sciences, v. 113, no. 3, p. 509-513.

478 Nesbitt, S. J., Sidor, C. A., Irmis, R. B., Angielczyk, K. D., Smith, R. M. H., and Tsuji, L. A.,

479 2010, Ecologically distinct dinosaurian sister group shows early diversification of

480 Ornithodira: Nature, v. 464, p. 95-98.

481 Nesbitt, S. J., 2011, The Early Evolution of Archosaurs: Relationships and the Origin of Major

482 Clades: Bulletin of the American Museum of Natural History, p. 1-292.

483   Nesbitt, S. J., Butler, R. J., and Gower, D. J., 2013, A new archosauriform (Reptilia: Diapsida)

484   from the Manda beds (Middle Triassic) of southwestern Tanzania: PLoS One, v. 8,

485   e72753.

486   Nesbitt, S. J., Sidor, C. A., Angielczyk, K. D., Smith, R. M. H., and Tsuji, L. A., 2014, A new

487   archosaur from the Manda beds (Anisian: Middle Triassic) of southern Tanzania and its

488   implications for character optimizations at Archosauria and Pseudosuchia: Journal of

489   Vertebrate Paleontology, v. 34, p. 1357-1382.

490   Nesbitt, S. J., Butler, R. J., Ezcurra, M. D., Barrett, P. M., Stocker, M. R., Angielczyk, K. D.,

491   Smith, R. M., Sidor, C. A., Niedźwiedzki, G., Sennikov, A. G. and Charig, A. J., 2017,

492   The earliest bird-line archosaurs and the assembly of the dinosaur body plan: Nature, v.

493   544, p. 484-487.

494   Ottone, E. G., Monti, M., Marsicano, C. A., Marcelo, S., Naipauer, M., Armstrong, R., and

495   Mancuso, A. C., 2014, A new Late Triassic age for the Puesto Viejo Group (San Rafael

496   depocenter, Argentina): SHRIMP U–Pb zircon dating and biostratigraphic correlations

497   across southern Gondwana: Journal of South American Earth Sciences, v. 56, p. 186-199.

498   Peecook, B. R., Steyer, J. S., Tabor, N. J., Smith, R. M., 2017, Updated geology and vertebrate

499   paleontology of the Triassic Ntawere Formation of northeastern Zambia, with special

500   emphasis on the archosauromorphs: Journal of Vertebrate Paleontology, 37(sup1), 8-38.

501   Polly, P. D., 2008, Adaptive zones and the pinniped ankle: a three-dimensional quantitative

502   analysis of carnivoran tarsal evolution, Mammalian evolutionary morphology: Dordrecht,

503   Springer, p. 167-196.

504   Qvarnström, M., Wernström, J. V., Piechowski, R., Tałanda, M., Ahlberg, P. E. and

505   Niedźwiedzki, G., 2019, Beetle-bearing coprolites possibly reveal the diet of a Late

506   Triassic dinosauriform: Royal Society Open Science, v. 6, p.181042.

507   Raup, D. M., 1979, Size of the Permo-Triassic bottleneck and its evolutionary implications:

508   Science, v. 206, no. 4415, p. 217-218.

509   Rubidge, B. S., 2005, 27th Du Toit Memorial Lecture: re-uniting lost continents–fossil reptiles

510   from the ancient Karoo and their wanderlust: South African Journal of Geology, v. 108,

511   no. 1, p. 135-172.

512   Sander, P. M., 1997,Teeth and jaws. Encyclopedia of dinosaurs, p. 717-725.

513   Santana, S. E., Strait, S., and Dumont, E. R., 2011, The better to eat you with: functional

514   correlates of tooth structure in bats: Functional Ecology, v. 25, no. 4, p. 839-847.

515   Scanlon, J. D., and Shine, R., 1988, Dentition and diet in snakes: adaptations to oophagy in the

516   Australian elapid genus *Simoselaps*: Journal of Zoology, v. 216, no. 3, p. 519-528.

517   Schluter, D., 1996, Ecological Causes of Adaptive Radiation: The American Naturalist, v. 148,

518   p. S40-S64.

519   Schoch, R. R., Ullmann, F., Rozynek, B., Ziegler, R., Seegis, D., & Sues, H. D., 2018, Tetrapod

520   diversity and palaeoecology in the German Middle Triassic (Lower Keuper) documented

521   by tooth morphotypes: Palaeobiodiversity and Palaeoenvironments, v. 98, p. 615-638.

522   Sidor, C. A., and S. J. Nesbitt., 2017, Introduction to vertebrate and climatic evolution in the

523   Triassic rift basins of Tanzania and Zambia; pp. 1–7 in C. A. Sidor and S. J. Nesbitt

524   (eds.), Vertebrate and Climatic Evolution in the Triassic Rift Basins of Tanzania and

525   Zambia. Society of Vertebrate Paleontology Memoir 17. Journal of Vertebrate

526   Paleontology 37 (6, Supplement).

527   Simpson, G. G., 1944, Tempo and Mode in Evolution, New York, Columbia University Press.

528   -, 1953, Major features of evolution, New York, Columbia University Press.

529   Smith, J. B., Vann, D. R., and Dodson, P., 2005, Dental morphology and variation in theropod

530   dinosaurs: implications for the taxonomic identification of isolated teeth: The Anatomical

531   Record, v. 285, no. 2, p. 699-736.

532   Smith, R. M., Sidor, C. A., Angielczyk, K. D., Nesbitt, S. J., and Tabor, N. J., 2018, Taphonomy

533   and paleoenvironments of Middle Triassic bone accumulations in the Lifua Member of

534   the Manda Beds, Songea Group (Ruhuhu Basin), Tanzania: Journal of Vertebrate

535   Paleontology, v. 37, no. sup1, p. 65-79.

536   Team, R. C., 2018, R: A Language and Environment for Statistical Computing.

537   Turner-Walker, G., 2008, The chemical and microbial degradation of bones and teeth: Advances

538   in human palaeopathology, v. 592.

539   Wickham, H., 2009, ggplot2: elegant graphics for data analysis, New York, Springer.

540   Wynd, B. M., Sidor, C. A., Whitney, M. R., and Peecook, B. R., 2018, The first occurrence of

541   *Cynognathus* in Tanzania and Zambia, with biostratigraphic implications for the age of

542   Triassic strata in southern Pangea. Vertebrate and climatic evolution in the Triassic rift

543   basins of Tanzania and Zambia: Society of Vertebrate Paleontology Memoir, v. 17, p.

544   228-239.

545   Zahradnicek, O., Buchtova, M., Dosedelova, H., and Tucker, A. S., 2014, The development of

546   complex tooth shape in reptiles: Frontiers in Physiology, v. 5, p. 74.

547   Zverkov, N. G., Fischer, V., Madzia, D., and Benson, R. B., 2018, Increased pliosaurid dental

548   disparity across the Jurassic-Cretaceous transition: Palaeontology, v.61, p. 1-22.

Figure 1

A sample of the *in situ* dental material used for baseline measurements in this study.

A – *Parringtonia* (NMT RB426) left dentary (left) in lateral (top) and medial (bottom) views and right dentary (right) in lateral and medial views. B – undescribed archosauriform taxon (NMT RB187) right maxilla in lateral and medial view. C – *Nundasuchus* (NMT RB48) holotype right dentary in lateral and medial views. D – *Asilisaurus* (NMT RB 837) (from left to right) right dentary in lateral and medial views, left maxilla in lateral and occlusal views, and right maxilla in lateral and occlusal views. Abbreviations: ap, ascending process of the maxilla; ds, dentary symphysis; ga, gastralia; mg, Meckelian groove; mt III, metatarsal III; nf, nutrient foramen; pp, palatal process. All scale bars 1 cm.
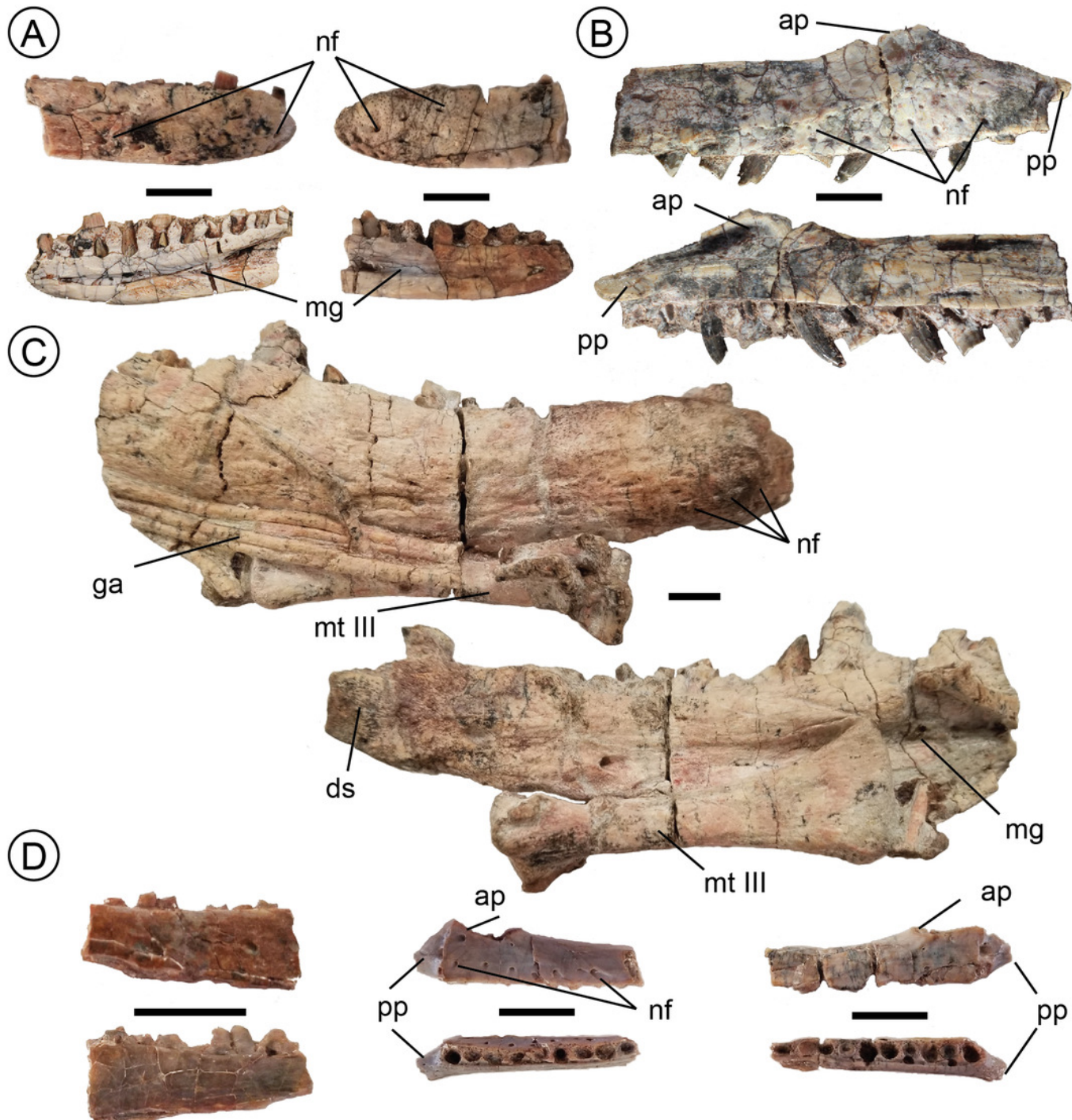
Figure 2

Examples of isolated teeth from the Manda Beds tooth assemblage.

A – Morphotype A specimens from left to right NMT RB807, NMT RB827, NMT RB809 in lateral and mesial views. Scale bars 1 cm. B – Morphotype B, specimens from left to right, NMT RB810, NMT RB819, NMT RB811 in lateral and mesial views. Scale bars 5 mm. C – sole representative of Morphotype C NMT RB831 in lateral and mesial views. Scale bar 1 cm. D – isolated teeth of known taxa. Top – *Nundasuchus* NMT RB48. Scale bar 1 cm. Bottom – *Parringtonia* NMT RB426 in lateral and mesial views. Scale bar 2 mm.
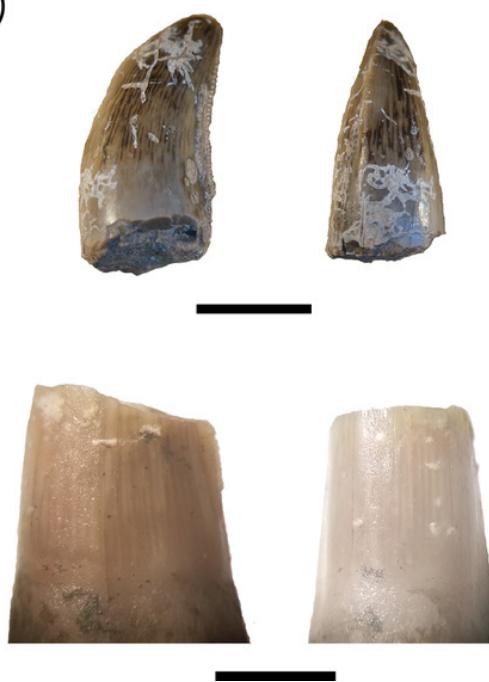
Figure 3

Visualization of discrete traits.

In all traits score 0 on left and score 1 on right. A – Trait 1, degree of recurvature, NMT RB819 (left) and NMT RB827 (right). B – Trait 2, fluting, NMT RB809 (left) and NMT RB426 (right). C – Trait 3, labiolingual curvature, NMT RB811 (left) and NMT RB819 (right). D – Trait 4, mesial margin angle, NMT RB811 (left) and NMT RB827 (right). E – Trait 5, labiolingual bulge, NMT RB811 (left) and NMT RB48 (right). F – Trait 6, dental caudae, NMT RB809 (left) and NMT RB810 (right). G – Trait 7, mesial vs distal serration series length, NMT RB831 (left) and NMT RB810 (right). H – Trait 8, denticle density per mm, NMT RB809 (left) and NMT RB810 (right), black lines equal 1 mm. I – Trait 9, mesial margin alignment, NMT RB810 (left) and NMT RB809 (right). J – Trait 10, mesial vs distal denticle density, NMT RB810 (left) and NMT RB809 (right). K – Trait 11, denticle shape variation along crown, NMT RB810 (left) and NMT RB48 (right).
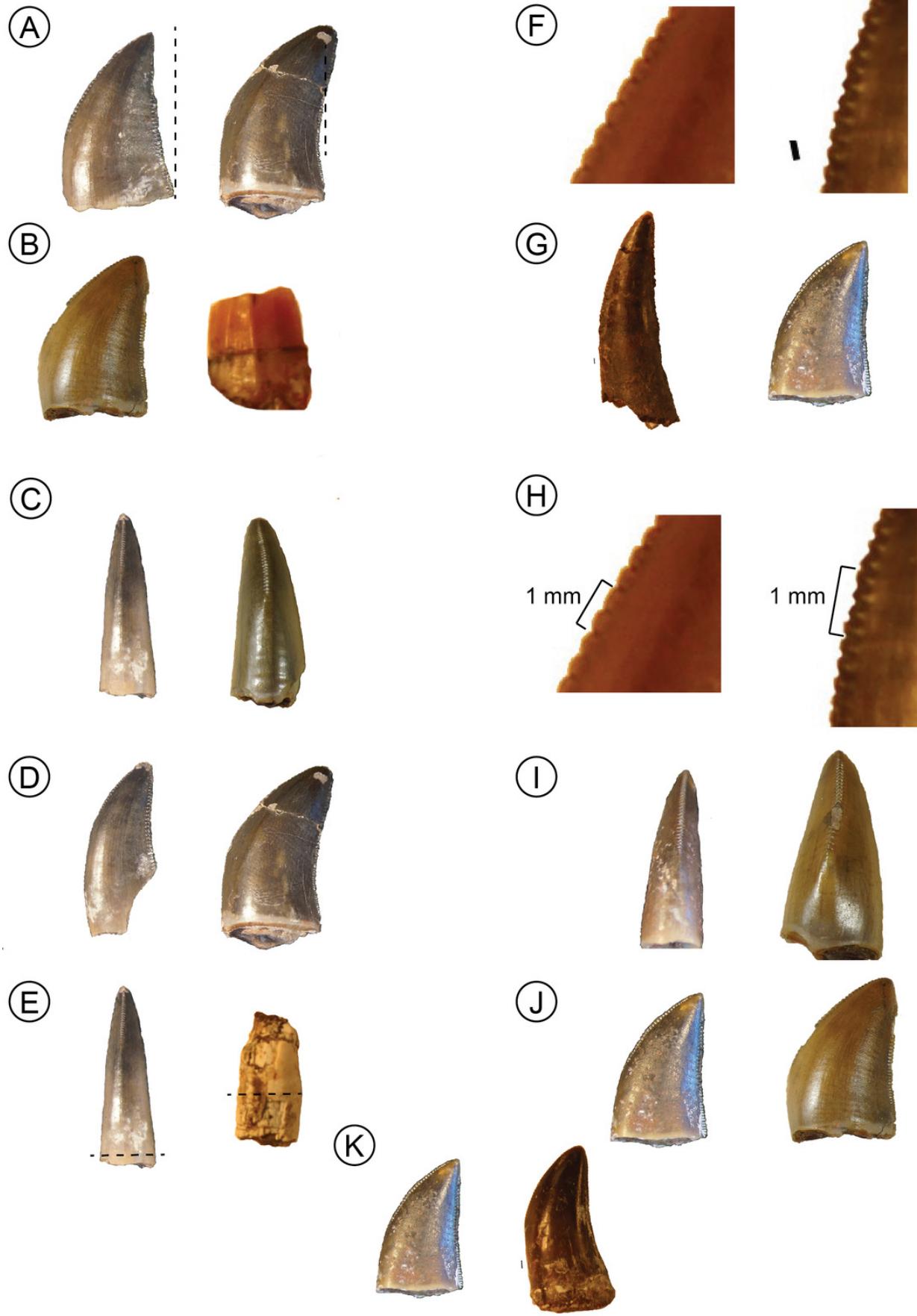
Figure 4(on next page)

Disparity of teeth measured by sum of variance

Disparity divided by taxon or morphotype. In the case of *Parringtonia* the two isolated teeth are an order of magnitude larger than the *in situ* teeth of this taxon, so this taxon was split. The sample sizes reflect the number of teeth with at least one of three measurements that was used to generate the predictive intervals.
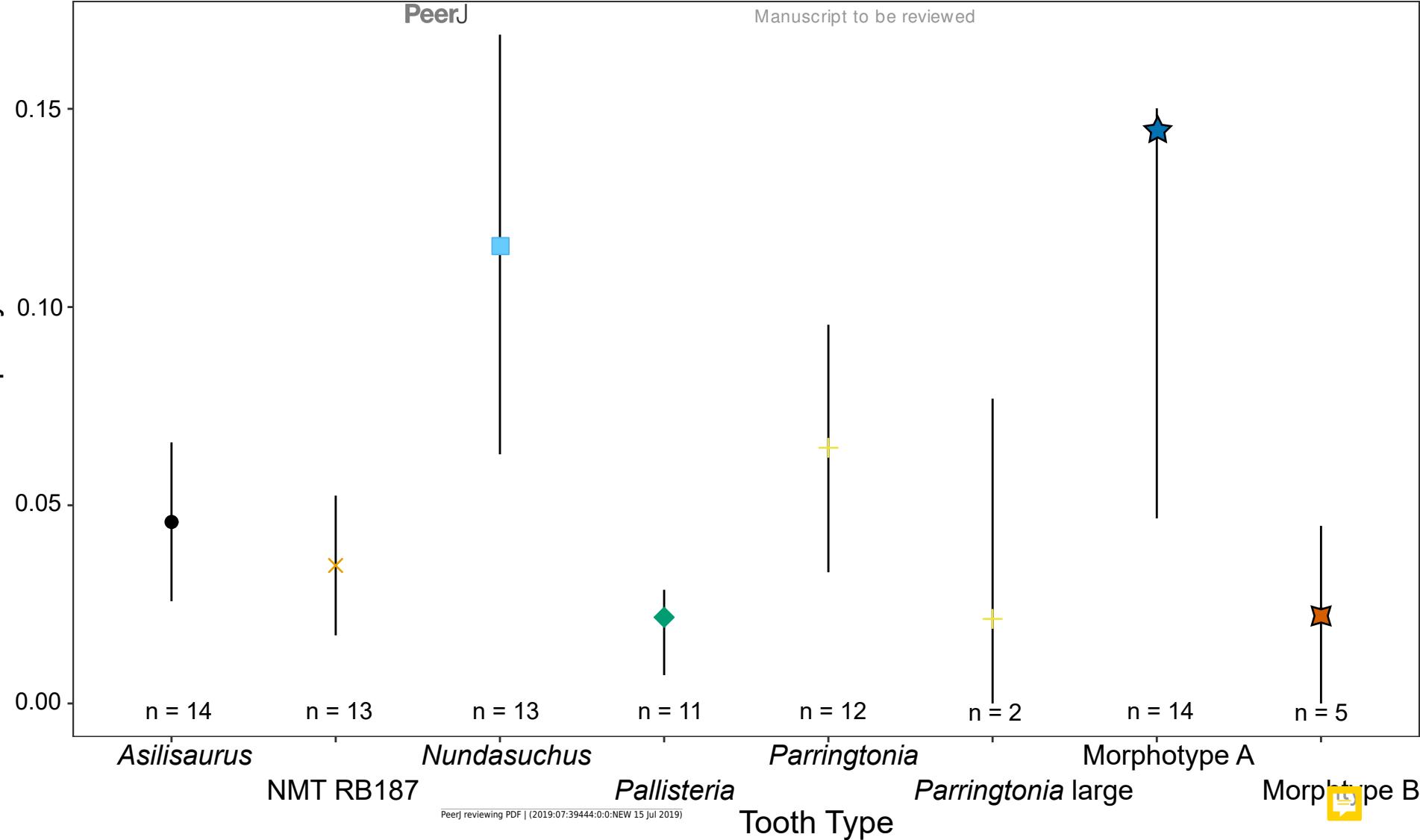
Figure 5(on next page)

Relationship between height and base shape of teeth divided by taxon.

The taxonomically unidentified teeth fall within a variety of the morphospaces generated by known taxa, rendering unambiguous referrals impossible. Some genera exhibit much greater variation in base shape ratio than others, potentially indicating a greater level of within-taxon variation.
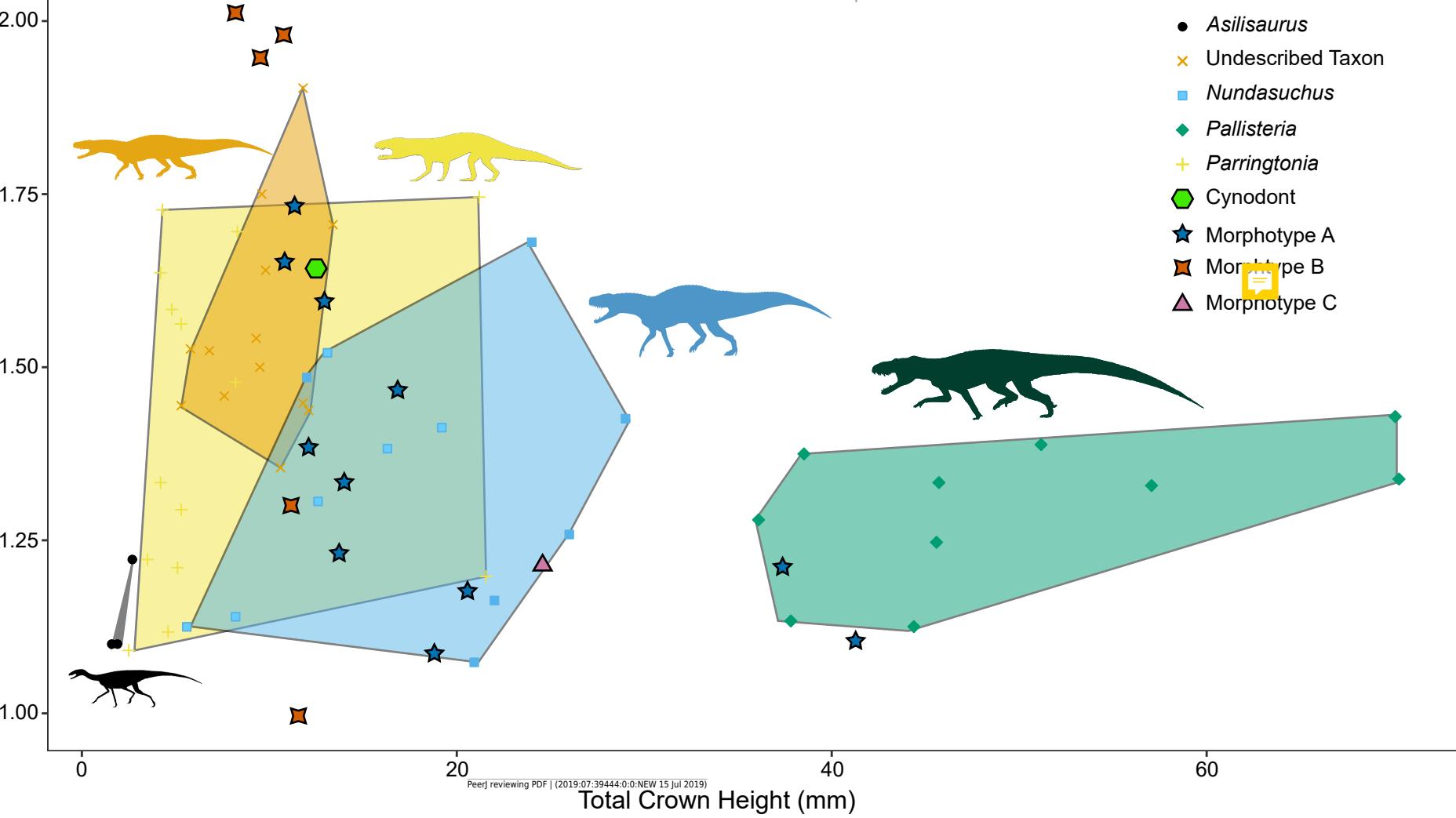
Figure 6(on next page)

Relationship between base width and fore-aft base length divided by taxon.

The overall ratio of base shape appears to be highly conserved with little deviation from the general trend. Differentiation between genera appears to be driven primarily by size.
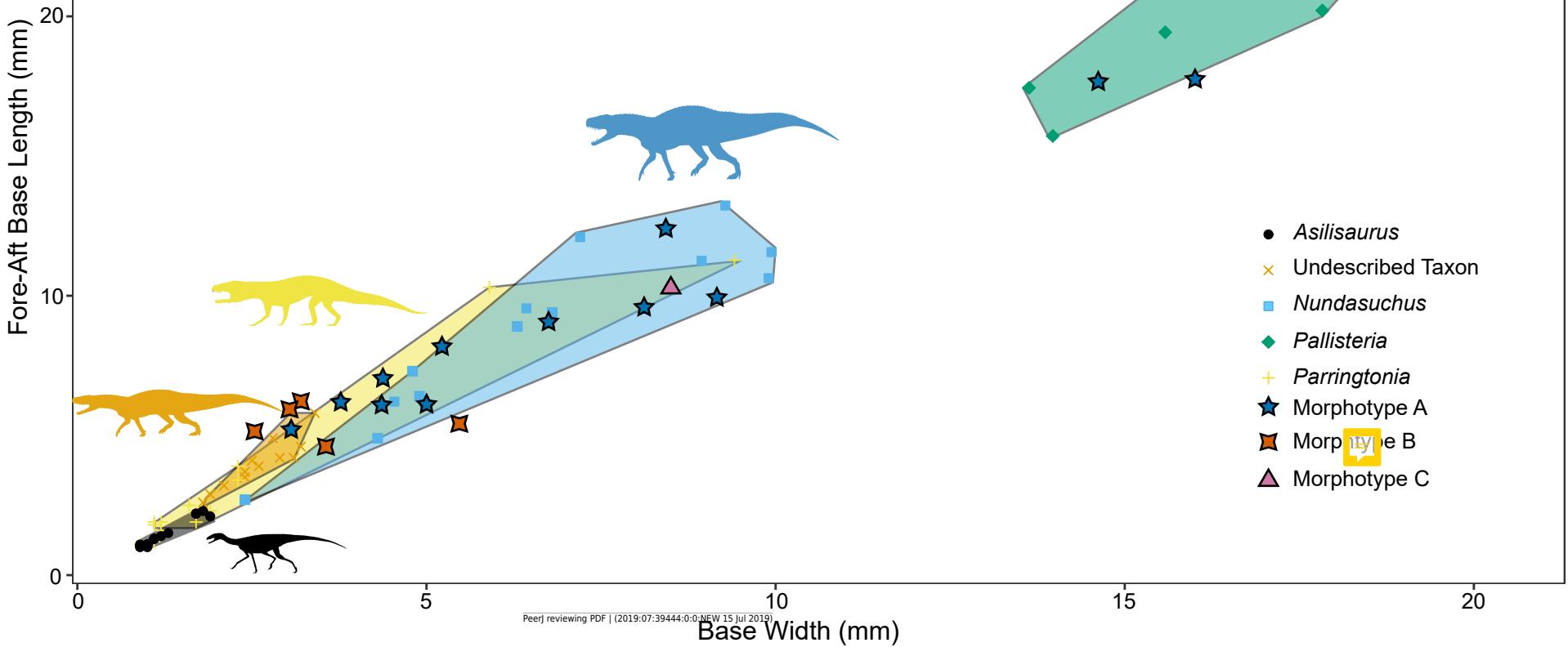
Figure 7(on next page)

Ordination plot of first two major NMDS axes of tooth morphospace.

Colored, transparent polygons represent the convex hulls of known taxa. Each point represents a separate tooth scoring. *Parringtonia* and NMT RB187 (undescribed taxon) share almost the same morphospace and there is substantial overlap between *Nundasuchus* and 'Pallisteria' also. Morphotype A appears to be more variable than Morphotype B, which is clustered closer together within a subsection of overall Morphotype A morphospace. The proximity of *Asilisaurus* to *Nundasuchus* and 'Pallisteria' is likely an artifact of incomplete scorings for *Asilisaurus* teeth.

NMDS 2

NMDS 1

- *Asilisaurus*
- Undescribed Taxon
- *Nundasuchus*
- *Pallisteria*
- *Parringtonia*
- Morphotype A
- Morphtype B
- Morphotype C
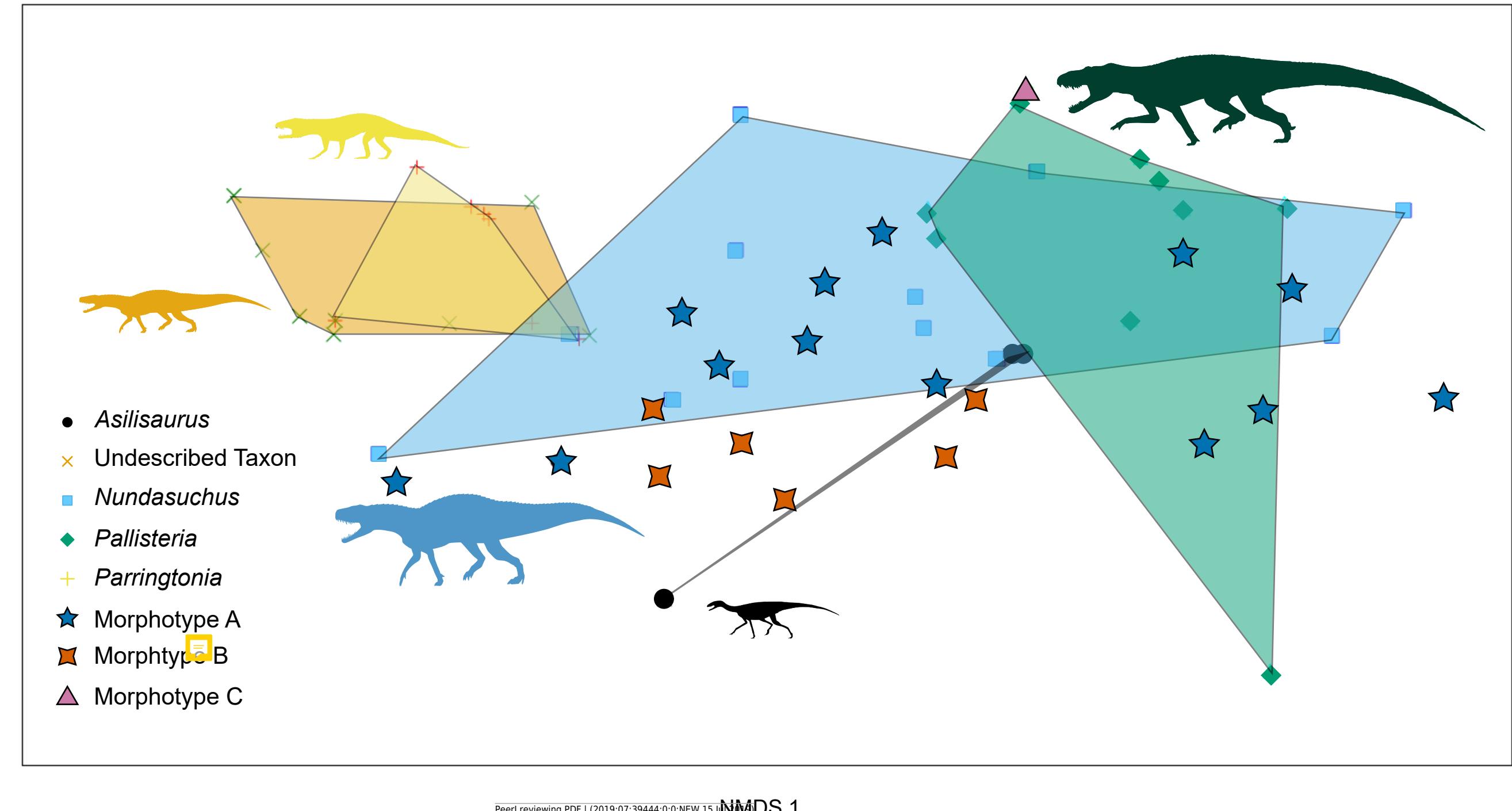
Figure 8(on next page)

Ordination plot of first two primary NMDS axes of tooth "averages" morphospace.

Taxa scoring represent "average" scores for each taxon. Only Morphotype C is represented by a single tooth. When using typical scores for taxa we find *Asilisaurus* is no longer near *Nundasuchus* and '*Pallisteria*' morphospace, but on the far side of ordination space.

NMDS 2

NMDS 1

Legend:
- ● *Asilisaurus*
- × Undescribed Taxon
- ■ *Nundasuchus*
- ◆ *Pallisteria*
- + *Parringtonia*
- ★ Morphotype A average
- ✦ Morphotype B average
- ▲ Morphotype C

Table 1(on next page)

Discrete character descriptions

Summary of the discrete, binary traits used for scoring teeth in the NMDS analysis.

	Description
1	Tooth apex, location, relative to the distal margin of the tooth base: tip mesial to or in the same vertical plane as the distal edge (0) or tip is located more distal than the distal edge (=recurved) (1)
2	Tooth lingual/labial, surfaces: texture is smooth (lack of crenulations, ridges, etc.) (0) or surface texture possess a series of parallel ridges from tooth apex to base (=fluted) (1)
3	Tooth labial/lingual, shape: crown curvature unequal (one side expanded relative to other) (0) or equal labial and lingual curvature (1)
4	Mesial tooth margin, shape: curvature angles change gradually (0) or angle changes abruptly at a single discrete point along mesial edge (1)
5	Tooth crown, size: labiolingual widths dorsal to the tooth crown base are all less than the crown base width (0) or a crown labiolingual width dorsal to the tooth crown base is greater than the crown base width (1)
6	Mesial/distal crown margins, surfaces: denticle caudae (= grooves on crown surface from between individual denticles) are absent (0) or present (1) (from Abler, 1992)
7	Mesial margin, length: mesial denticle row ends at a point sub-equal with distal denticle row (0) or mesial denticle row ends significantly further apically on crown than distal row (1). Can only be scored for teeth with both mesial and distal denticle series.
8	Mesial/distal margins, denticle density: number of mesial and distal denticles is < 3 per mm (0), or greater than or equal to 3 per mm (1). Measurements are taken near the middle of the carina.
9	Mesial margin, location: vertical axis of the mesial carina is in line the mesial-distal long axis (0) or laterally offset from the mesial distal long axis (1)
10	Mesial/distal margins, size: average size of mesial and distal denticles are the same (0) or the average size of the mesial and distal denticles is different (1)
11	Mesial/distal margins, shape: lateral profile shape of mesial and distal denticles remains constant (0) or denticles' lateral profile changes shape (e.g. rounded to square) (1)

1

Table 2(on next page)

Results of linear model (base ~ total crown height + taxon)

All measures of significance are calculated in reference to the intercept, *Asilisaurus*.
Therefore, while the undescribed pseudosuchian and *Parringtonia* can be differentiated in the
model from *Asilisaurus*, the interrelationships are unknown.

	Estimate	Standard Error	t-value	p-value
Asilisaurus (intercept)	1.1285	0.1011	11.156	<0.0001
Total Crown Height (mm)	0.0059	0.0035	1.714	0.0933
Undescribed	0.3718	0.1148	3.237	0.0022
Nundasuchus	0.0995	0.1247	0.798	0.4290
'Pallisteria'	-0.1249	0.2007	-0.622	0.5369
Parringtonia	0.2490	0.1127	2.210	0.0321

1

Table 3(on next page)

Pairwise comparisons of taxa used in the linear model.

The undescribed pseudosuchian is readily differentiable from most taxa, with the exception of *Parringtonia*. Confidence intervals were generated using a 95% confidence level.

Taxon	lsmeans	Standard Error	df	Lower CL	Upper CL
Asilisaurus	1.2354	0.1150	46	1.0039	1.4669
Undescribed	1.6071	0.0568	46	1.4929	1.7214
Nundasuchus	1.3348	0.0505	46	1.2332	1.4365
'Pallisteria'	1.1105	0.1225	46	0.8640	1.3570
Parringtonia	1.4844	0.0595	46	1.3645	1.6042

1

Contrast	Estimate	SE	df	t ratio	p-value
Asilisaurus – Undescribed	-0.3718	0.1148	46	-3.237	0.0181
Asilisaurus – *Nundasuchus*	-0.0995	0.1247	46	-0.798	0.9299
Asilisaurus – *'Pallisteria'*	0.1249	0.2007	46	0.622	0.9708
Asilisaurus – *Parringtonia*	-0.2490	0.1127	46	-2.210	0.1944
Undescribed – *Nundasuchus*	0.2723	0.0751	46	3.625	0.0062
Undescribed – *'Pallisteria'*	0.4967	0.1571	46	3.162	0.0222
Undescribed – *Parringtonia*	0.1228	0.0677	46	1.813	0.3788
Nundasuchus – *'Pallisteria'*	0.2244	0.1343	46	1.671	0.4614
Nundasuchus – *Parringtonia*	-0.1495	0.0770	46	-1.942	0.3107
'Pallisteria' – *Parringtonia*	-0.3739	0.1631	46	-2.292	0.1659

2